

# Surface Boundary Layer Atmospheres

R.E. Johnson

*Engineering Physics and the Department of Astronomy, University of Virginia*

The solar system contains many bodies with atmospheres so thin that collisions seldom occur between the atmospheric constituents. These are called surface boundary layer atmospheres. Not only is the surface the source of the atoms and molecules, but their interactions with the surface determine the atmospheric properties. These atmospheres are interesting for two reasons. By remote sensing we can learn about the external weathering agents and we may also be able to determine the surface compositions of distant bodies. Here the physical processes that control these atmospheres are described and our knowledge of the surface boundary layer atmospheres in the solar system is reviewed.

## 1. INTRODUCTION

The solar system contains many small bodies with tenuous atmospheres, some so thin that the atoms and molecules leaving the surface collide only rarely if at all. In this situation the properties of the atmosphere, or ambient gas, are dominated by the interactions of the constituent atom and molecules with the surface and by loss to space. Such atmospheres are also called exospheres because atoms leaving the surface can directly escape as they do from planetary exospheres (see II.2). When collisions can be neglected, the atmosphere is a sum of independent components each characterized by a surface ejection process. Such atmospheres are referred to here as surface boundary layer atmospheres since the interactions with the surface determine the composition and density.

These atmospheres are derived from the intrinsic planetary materials, impacting materials or implanted ions. Therefore, remote sensing observations can lead to an understanding of the surface composition and the weathering processes [Johnson and Sittler, 1990; John-

son and Baragiola, 1991]. Although this is an important goal, it typically founders on our lack of understanding of those processes which lead to desorption of atoms and molecules from the surface. Desorption from a surface can occur due to thermal processes and micrometeorite impact vaporization, and it is induced by incident photons, electrons and ions. Each of these processes is not well understood for the materials composing the porous regoliths of solar systems bodies. Good observations, therefore, are often accompanied by essentially speculative models due to the lack of laboratory data or reliable models for desorption.

The Mariner and Apollo missions showed that both Mercury and the Moon had extremely rarefied atmospheres. The sources were primarily solar wind implantation of hydrogen and helium, rare gas atoms produced by radioactive decay and nuclear reactions induced by cosmic ray particles, and, possibly, some sputtered oxygen. Renewed interest in these atmospheres was generated by the observation of ambient alkali atoms, first at Mercury and then at the Moon [Potter and Morgan, 1985, 1986, 1988]. This led to new modeling and observational efforts with the hope that remote sensing could be used to compare the composition of the surfaces of the Moon and Mercury. However, additional species were not identified until the recent observation of Ca at Mercury [Bida *et al.*, 2000].

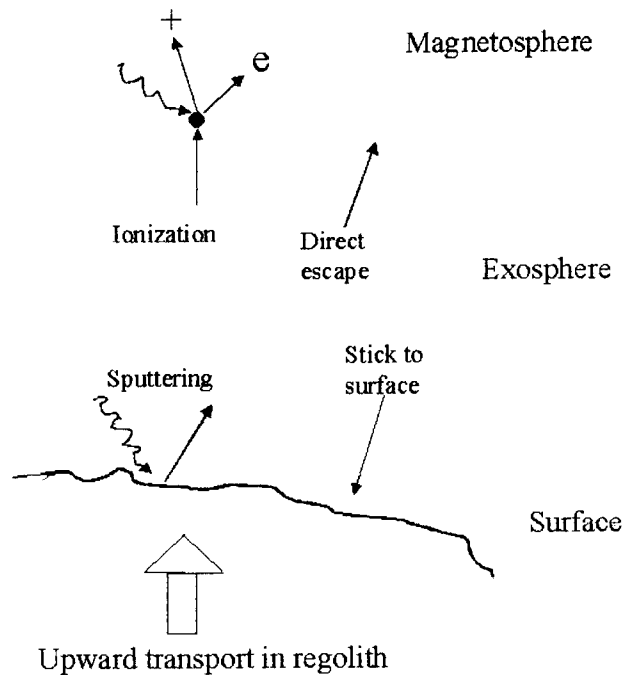


**Figure 1.** Source and loss processes determining the nature of the surface boundary layer atmospheres [Cheng *et al.*, 1987].

A parallel story for outer solar system bodies had been evolving for  $\sim 20$  years. Subsequent to the first observation of sodium at Io [Brown and Chaffee, 1974], Voyager found that a number of the large moons of the giant planets had extremely thin, exospheric atmospheres. It also confirmed that many of these surfaces were composed primarily of frozen volatiles and were embedded in relatively intense fluxes of charged particles trapped in the giant planet magnetospheres. Based on laboratory data for sputtering of ices, these moons were predicted to have thin atmospheres [Cheng and Lanzerotti, 1974]. Because water ice is decomposed by energetic plasma particles [Reimann *et al.*, 1984], the icy moons were also predicted to have  $O_2$  atmospheres [Johnson *et al.*, 1982; Johnson, 1990]. These predictions were both confirmed. An ambient cloud of OH was observed at Saturn by HST [Shemansky *et al.*, 1993], derived in part from  $H_2O$  escaping from the icy satellites, and  $O_2$  was detected by 'auroral' emissions at Europa and Ganymede [Hall *et al.*, 1998]. There is now considerable excitement that atmospheric observations can give information on the evolution of Europa's surface [Johnson *et al.*, 1998] and on its ocean which has breached the surface in the past [Pappalardo *et al.*, 1999]. Alkali atoms seen in Europa's atmo-

sphere [Brown and Hill, 1996] were suggested to have come from ocean material [Johnson, 2000; Brown, 2001; Leblanc *et al.*, 2001] and the search is on for other species that might suggest whether biology was initiated in Europa's ocean [Chyba, 2000].

In this Chapter, I first review the ejection and transport processes that determine the atmospheric properties. Because of the existence of a number of good reviews [Hunten *et al.*, 1988; Hunten and Sprague, 1997; Stern, 1999; Killen and Ip, 1999], I will only briefly describe our present understanding.

## 2. PHYSICAL PROCESSES

An atom or molecule ejected from the surface moves in a ballistic trajectory, primarily under the influence of the body's gravitational field as seen in Figure 1. If it has sufficient energy it can escape, it can be ionized and lost, or ionized and swept into the surface by the local fields [Manka and Michel, 1973; Goldstein *et al.*, 1981]. Neutrals which do not escape or are not ionized return to the surface. Ejected molecules can be dissociated with their fragments following escape or bound trajectories. The contribution of these atoms and molecules to the observed density depends on the flight time, which in turn depends on its initial ejection velocity. Those particles which return to the surface ballistically or return by being ionized and swept into the surface can again be ejected. A refinement to this picture is the interaction with the radiation field. An effective pressure is produced by resonant scattering [Smyth and Marconi, 1995] or by collisions with the plasma particles [Jurac *et al.*, 2000]. For long flight paths, collisions with other neutrals can become relevant. An atmosphere in which collisions are important can exhibit characteristics of a surface boundary layer atmosphere if its properties are determined primarily by the interactions with the surface. Finally, each body has atmospheres at two scales: a planetary scale ambient gas above the physical surface in equilibrium with a micro-scale atmosphere in the regolith [Hodges, 1980].

The word source sometimes refers to the ejection process and other times to the reservoir of the observed atoms and molecules. These are the same for venting. Here I describe ejection processes and use the word source for the reservoir. Internal (endogenic) sources of atmosphere must be replenished by regolith turnover, outgassing or diffusion. External (exogenic) sources include implantation of ions from the local plasma, impacting meteoroids and comets, or ejecta from a neighboring object. The ejection and transport processes are described below.

## 2.1. Thermal Processes

Outgassing can produce a tenuous atmosphere controlled by condensation and loss to space. This can be a robust process, like volcanoes at Io or venting at Triton. The ejecta velocity distributions are determined by the temperature of the reservoir and by collisions in the expanding plume. At some distance from the source, the atmosphere becomes a thin boundary layer atmosphere. Bodies might also outgas by slow, steady thermal diffusion as suggested for the CO<sub>2</sub> at Callisto [Carlson, 1999]. Modeling requires accounting for the source rates and the velocity distributions.

Trace atoms or molecules which are bound to or adsorbed on the surface (e.g., Ar at night on the Moon) can be desorbed thermally. The rate of ejection is proportional to their surface concentrations,  $c_j$ , to their vibrational frequency on the surface,  $\nu_j$  ( $\approx 10^{13}/s$ ) and an exponential function of their surface binding energy,  $U_j$ :  $dS/dt \approx c_j \nu_j \exp[-U_j/kT]$ . Thermally desorbed species that are fully accommodated have a roughly Maxwellian velocity distribution, typically given as a normalized flux distribution,  $f(E, \theta) = [2\cos\theta][E/(kT)^2] \exp(-E/kT)$ .

In the subsolar region, sublimation can be important on the frozen surfaces in the outer solar system. Whereas thermal desorption refers to ejection of a trace species, like Na at Mercury, sublimation describes ejection of the principal species such as H<sub>2</sub>O at Ganymede. The velocity distribution is typically like that above and the flux is determined from the vapor pressure at the surface,  $P(T, x)$ , and the sublimation energy  $U$ :  $\Phi = c[P(T) / (2\pi M kT)^{1/2}] \exp(-U/kT)$ . The prefactor is related to  $\nu_j$  above and the coverage,  $c$ , can account for porosity.

## 2.2. Stimulated Desorption and Sputtering

Whereas the solar photon flux heats the surface, determining the thermal desorption efficiencies, individual photons can excite a bond in the surface [Madey et al., 2001]. This can lead to repulsive ejection of an atom or molecule, referred to as photon stimulated desorption or photo-sputtering. These terms have been used interchangeably but typically refer to removal of a trace or adsorbed species vs. removal of the principal species. Stimulated desorption is less robust than thermal desorption but becomes important when  $\exp[-U_j/kT]$  is small. The dominant ejecta are neutrals. Ion ejection requires higher energy excitations (typically  $> \sim 25\text{eV}$ ) but as they are easy to detect the literature is predominantly on ion desorption. Because ejected ions

contribute directly to the local plasma, they might at times be important, but most observed plasma ions are formed from ejected neutrals.

CO is desorbed by exciting states of internal molecular bond of CO or by exciting a state associated with the molecule / surface bond [Madey et al., 2001]. These can be quenched or they can lead to repulsive ejection. Exciting a surface state can lead to ejection of a CO whereas the internal states lead to ejection of an atom, typically the O. Adsorbed or intrinsic Na is bound in an ionic form to a silicate [Yakshinskiy and Madey, 2000]. An incident photon can excite an electron which attaches to the sodium causing ejection [Yakshinskiy and Madey, 1999]. The threshold for alkali atom desorption from a silicate or an icy surface is only a few eV [Yakshinskiy and Madey, 1999, 2001]. The desorbed flux,  $\Phi_j$ , for species  $j$  can be written as  $\Phi_j = \eta_j \sigma_j^{des} \phi$ , where  $\phi$  is the incident photon flux,  $\sigma_j^{des}$  is the desorption cross section and  $\eta_j$  is the number per unit area in the surface. The quantity  $(\eta_j \sigma_j)$  is also called the yield. The cross section  $\sigma_j^{des}$  is the product of an absorption cross section for the photon and the probability of ejection. Whereas gas-phase photo-absorption cross sections for outer shell electrons range from  $\sim 10^{-17}$ - $10^{-19}\text{cm}^2$ , desorption cross sections can be an order of magnitude or more smaller due to the quenching of the excitations in the solid. Whereas ejected ions can have average energies  $\gg 1\text{eV}$ , the ejected neutrals have average energies  $< 1\text{eV}$ . Stimulated desorption is non-thermal but can have a quasi-thermal component due to the interaction of the exiting atom with other surface atoms. Since planetary surfaces are porous, a thermal distribution with an energetic tail is appropriate.

Adsorbed water can be typically dissociated by incident UV photons, [Kimmel et al., 1995] If this occurs at the vacuum interface, H or H<sub>2</sub> is directly ejected and H<sub>2</sub> produced at depth diffuses out. For a vapor deposited ice, which is very rough at the molecular level, weakly attached water molecules can be directly desorbed [Bahr et al., 2000]. However, removal of H<sub>2</sub>O typically requires two photons [Westley et al., 1995]. The first causes the loss of H or H<sub>2</sub>, producing a precursor species: e.g., trapped OH or O [H<sub>2</sub>O·O]. Subsequent excitation of the precursor can lead to desorption [Sieger et al., 1998]. Therefore, the yield is roughly quadratic in the radiation flux,  $\phi$ , and is temperature dependent.

Fast ions and electrons ( $> \sim 10^7\text{cm/s}$ ) from the local plasma can cause desorption and sputtering by electronic excitations, a process referred to as electronic sputtering [Johnson, 1996]. If the density of excitations produced near the surface is low, as is the case

for incident electrons and fast protons, then electronic sputtering resembles photo-desorption [Johnson, 1990]. However, the fast heavy ions in the Jovian magnetospheric plasma [Cooper *et al.*, 2001] produce high excitation densities leading to large sputtering yields in ice. The yields for a number of relevant ices are often parametrized by the square of the energy deposited per unit path length in excitations and ionizations,  $(dE/dx)_e$  [Johnson, 1990, 1998; Shi *et al.*, 1995], a tabulated quantity. The ejecta spectrum is not Maxwellian. It has an average energy  $<1\text{eV}$ , but with a slowly decaying tail,  $\sim E^{-2}$  [Johnson, 1990], and is often parametrized using  $f(E) = 2EU'/(E + U')^3$ , where  $U'$  is a fitting parameter which is typically low,  $<0.1\text{eV}$ .

Incident plasma ions also transfer energy to surface atoms in 'knock-on' collisions [Johnson, 1990; 1998]. This is the standard sputtering process which leads to non-selective ejection. It is the dominant ejection process in most refractory solid and is most efficient at energies  $\sim 0.1\text{--}1\text{keV/u}$ . It has the hardest spectrum with the parameter  $U'$  above related to the cohesive energy of the material,  $U$ . It is the most discussed sputtering process, but has not yet been shown to be dominant on any object. Although there is a large body of data and good computational tools for knock-on sputtering, details for planetary materials are sparse.

Micrometeorite impact vaporization of regolith grains and the impactor has been suggested as an atmospheric source at the Moon [Morgan *et al.*, 1989], Mercury [Morgan *et al.*, 1988; Hunten *et al.*, 1988], and Enceladus [Haff and Eviatar, 1986]. Micrometeorites, which produce the porous regoliths and convert lunar surface materials into glasses, also mix the surface exposing fresh material. The vapor coats lunar grains [Hapke, 2001] and can produce an enhancement in the sodium atmosphere during meteor showers [Hunten *et al.*, 1998; Smith *et al.*, 1998]. The ejecta exhibit a Maxwellian-like velocity distribution and the amount of material vaporized per impact is of the order of a few times the mass of the impactor. The porous regolith produced by micrometeorite bombardment can severely reduce the sputter flux by shadowing and sticking of ejecta to neighboring grains [Hapke, 1986; Johnson, 1989].

### 2.3. Radiolysis and Photolysis: Chemical Sputtering

The incident charged particles and photons also induce chemistry called radiolysis and photolysis [Johnson and Quickenden, 1997]. The surface is altered down to the depth of penetration by implantation of reactive species (e.g., H, C, O and S) and by bond breaking. That radiolysis occurs on the icy moons is indicated by the

observation of peroxide [Carlson *et al.*, 1999b]. In radiolysis and photolysis new more volatile species are created which preferentially desorb, often called chemical sputtering [Roth, 1983]. For instance, ice is decomposed into  $\text{H}_2$  and  $\text{O}_2$  [Reimann *et al.*, 1984] and protons and carbon implanted into the lunar regolith can form  $\text{CH}_4$ . Volatiles produced at depth can diffuse to the surface (e.g.,  $\text{H}_2$  from  $\text{CH}_4$  [Lanzerotti *et al.*, 1987]) and escape with a thermal energy distribution. In some materials the loss of volatiles leaves a less volatile surface, as is the case for vapor deposited  $\text{SO}_2$  irradiated in Io's polar regions producing sulfur chains [Johnson, 1997]. Similarly, outer solar system surfaces containing hydrocarbons preferentially lose H (as  $\text{H}_2$ ) forming carbon chains [Strazzulla, 1998] and many organic molecules decompose yielding  $\text{CO}_2$  and darker material, a process possibly relevant at Callisto [Johnson, 2001]. The chemistry can be induced by hot atom reactions, but most measured yields vary with the surface temperature [Johnson, 1990, 1998]. These chemical changes compete with regolith turnover and vapor deposition in determining the surface reflectance.

### 2.4. Adsorption

Ejected atoms and molecules returning to the surface typically do not reflect efficiently, since their velocities are low and the surfaces are porous. If they do scatter back into the gas phase before fully accommodating to the surface temperature, their average energy is characterized by a coefficient,  $\beta = [E_{out} - E_j]/[E_T - E_{in}]$ , where  $E_{in}$  and  $E_{out}$  are the incident and re-ejection energies and  $E_T$  is the thermal energy [Hunten *et al.*, 1988]. Since natural surfaces are highly porous, full accommodation to the local temperature is a good assumption for all except the lightest atoms, H and He [Hodges, 1974; Shemansky and Broadfoot, 1977]. That is, the returning atoms or molecules become adsorbed weakly on the surface (physisorbed;  $U_j \ll 1\text{eV}$ ). In this state they can migrate along the surface of a grain until they find a deep adsorption or reaction (chemisorbed) site or desorb thermally. Therefore, with the exception of H and He, returning particles essentially stick ( $\beta \approx 0$ ) with a residence time that depends on the surface temperature and the availability of deep sites [Smith and Kay, 1997; Yakshinskiy and Madey, 2000]. These are available on surfaces in a clean space environment [Hodges, 2001] and are produced by radiation damage [Yakshinskiy and Madey, 1999].

In laboratory studies a distinction can be made between direct reflection, sticking-migration-desorption, and sticking and becoming bound in a deep well [Smith

and Kay, 1997]. In modelling, one typically uses a net sticking coefficient,  $S$ , which combines the probability of physisorption and the probability of finding a binding site. For He there are no deep sites, but even Ar can bind at night on clean lunar grains [Hodges, 2001]. Water has a high apparent sticking coefficient on MgO. It chemisorbs molecularly at terrace sites and dissociatively at radiation damage sites. Interestingly, the thermal activation energy in both cases is  $\sim 63\text{kJ/mole}$  [Stirniman *et al.*, 1996]. Yakshinskiy *et al.* (2000) give the net sticking for Na on a silicate:  $S \approx 0.5$  at 250K decreasing to 0.2 at 500K. The Na absorbed on an amorphous silicate has binding energies ranging from  $\sim 1.4\text{eV}$  to  $2.7\text{eV}$  with a peak  $\sim 1.85\text{eV}$ , greater than the  $1.1\text{eV}$  suggested earlier [Hunten and Sprague, 1997]. At 500K the resident time on a grain at the average binding energy is  $\sim 13$  hours and at 400K it becomes  $\sim 103$  yrs.

Since the grains form a regolith, desorbed molecules intersect a surface with high probability prior to contributing to the ambient gas. The atoms and molecules hopping between grain surfaces create an regolith atmosphere in equilibrium with the observed ambient gas. The net sticking coefficients in a regolith is  $S_{eff} \approx S/[1-(1-S)(1-P)]$  where  $P$  is the probability of escape. For isotropic ejection,  $P$  is  $\sim 0.2$  [Hodges, 1980a; Johnson, 1989]. Therefore, at 250K and 500K,  $S_{eff}$  is  $\sim 0.8$  and  $\sim 0.6$ , close to the value found when modeling observations [Sprague, 1992].

### 2.5. Interaction With the Radiation Field

The atoms and molecules in their ballistic trajectories can interact with the local radiation field. This can lead to excitation, ionization and dissociation of molecules as well as momentum transfer. The interaction of solar photons with the alkali atoms has been extensively described [Smyth and Marconi, 1995a]. The strong resonance scattering lines which allow trace amounts of Na and K to be studied from earth produce an average acceleration away from the sun. That is, an atom absorbs a photon receiving a momentum directed away from the sun and then re-emits in a random direction giving up some momentum. Instead of treating this stochastically, it is treated as a radiation pressure, since each event transfers a small amount of momentum and the ballistic lifetimes are generally longer than the resonant scattering time. Although a small effect, the pressure is steady, driving sodium and potassium atoms in large ballistic orbits downstream from the sun [Wilson *et al.*, 1998]. The ability to absorb is affected by the atom's radial motion relative to the sun which causes a Doppler

shift. Since Mercury is both close to the sun and in an eccentric orbit, the net acceleration can vary considerably depending on Mercury's orbital position [Smyth and Marconi, 1995a].

Interaction with the plasma can also produce a net drag via momentum transfer to atmospheric neutrals producing, for instance, an expansion of Saturn's OH torus [Jurac *et al.*, 2000]. Since the size of the momentum transfer can be large this is typically treated stochastically. When such collisions lead to removal of a molecule from an atmosphere, it is often called atmospheric sputtering [Johnson, 1990].

Ionization by photons, electron impact, or charge exchange are important loss processes for a number of the surface boundary layer atmospheres. Estimating the loss requires knowledge of the plasma flux and the ionization and charge exchange cross sections. A useful quantity is the average lifetime against ionization,  $\tau_i = [\phi \sigma_i]^{-1}$ , where  $\sigma_i$  is the ionization cross section and  $\phi$  is the radiation flux. Photoionization cross sections integrated over the solar spectrum are available for many atmospheric species [Huebner *et al.*, 1992] and plasma cross section data, though not always available, can be reasonably estimated [Johnson, 1990]. The biggest uncertainty is knowledge of the plasma density and temperature, especially close to the body. The interaction of the external field with the local field can be variable [Ip, 1986; Kabin *et al.*, 2000] and ionization followed by pick-up produces a current. This current in turn deflects the plasma flow, as modeled for Europa's O<sub>2</sub> atmosphere [Ip, 1996; Saur *et al.*, 1998]. Accurately calculating the feedback is not trivial but is important at the Jovian satellites and Mercury.

### 2.6. Transport and Recycling

Particles desorbed from the surface move in ballistic trajectories usually calculated in the coordinate system of the body. When no outside forces act, the radial gravitational force,  $\mathbf{F}_G$ , controls the motion. However, if the radiation pressure and/or the gravitational force of the sun or of a parent planet (e.g., Jupiter for Europa) is significant, then motion of the body is important and Coriolis and centrifugal forces must also be included (see III.4).

When considering only  $\mathbf{F}_G$  and ignoring losses, the ejecta energy distribution,  $f(E, \theta)$  determines atmospheric transport and escape, where  $E$  and  $\theta$  are the energy and angle. The escape fraction,  $f_{es}$ , is obtained by integrating over energies greater than  $U^S$ , the satellite gravitational energy. For surface boundary layer atmospheres transport is always important since stimulated

and thermal desorption exhibit longitudinal and latitudinal dependences. For outer solar system moons phase-locked to their parent planets and moving in the magnetospheric plasma, there are differences in the bombardment flux onto the hemispheres leading and trailing the orbital motion [Pospieszalska and Johnson, 1989; Paranicas et al., 2001]. This produces differences in the ejected flux so that trace species are moved poleward or, in the case of the Jovian satellites, to the leading hemisphere [Sieveka and Johnson, 1982]. When ejection depends on temperature there is a net poleward and day to night transport, so that Ar at the moon exhibits daily transients [Hodges, 1980a]. If the molecules are fully accommodated to the local surface temperature, then thermal desorption and adsorption events lead to a random walk across the surface and into the regolith. When hopping distances are small, the process is roughly diffusive [Hodges, 1974].

Ignoring loss processes, the angular excursion across the surface and the mean flight time,  $t_b$ , in a bound trajectory are easily estimated [Johnson, 1990]. The averages are obtained by integrating over the energy and angle distribution of the ejecta for the bound trajectories. When  $t_b \ll \tau_i$  and ejection is isotropic, the column is  $\Phi_j \cdot t_b$ , where  $\Phi_j$  is the flux discussed earlier. For sputtering of H<sub>2</sub>O at Europa the escape fraction is  $f_{es} \approx 0.3$ , the mean angular excursion is  $\sim 50^\circ$ , indicating relatively large ballistic trajectories, and the mean flight time is  $\sim 4 \times 10^3$  s [Johnson, 1990]. For O<sub>2</sub> at the ambient temperature on Europa's dayside hemisphere ( $\sim 120$  K) the escape fraction is nearly zero, the mean excursion angle is  $\sim 2^\circ$  and the mean flight time is shorter,  $\sim 200$  s. Both of these times are short compared to the lifetime against ionization,  $\tau_i \approx 10^6$  s. Therefore, most particles in bound trajectories return to the surface. If gas-phase ionization is the only loss process and if the residence time on the surface is short then the average number of hops across the surface is  $\bar{N} \approx \tau_i / \langle t_b \rangle$ . The mean excursion distance for a Maxwellian flux distribution is  $\sim \pi H_j$ , where  $H_j$  is the scale height,  $H_j = kT/M_j g$ . For the sputter energy distribution above, the mean excursion distance depends on the cut-off,  $E_{max}$ , which is typically not measured. For  $E_{max}/U_j' \gg 1$ , this gives  $\sim \pi H_j^c \ln(E_{max}/U_j')$ . For a 2-D random walk with an average of  $\bar{N}$  hops, the mean radial distance traveled before removal is  $\sim \pi H_j [\bar{N}]^{1/2}$ . This is of the order of Europa's radius for O<sub>2</sub> near the dayside equator.

Finally, ionized species follow the local field lines and can be re-implanted into the surface [Manka and Michel, 1973; Cheng et al., 1987]. This produces poleward transport in the local dipole field at Ganymede or

Mercury. Because of Mercury's slow rotational period, it has been suggested [Sprague, 1992] that this could produce a net transport process from dayside to the nightside allowing recycling of the alkalis.

### 2.7. Density Calculations

The density vs. altitude depends on the surface ejection rate, the ballistic flight time,  $t_b$ , and the loss processes. Atoms and molecules ejected from the surface have a residence time in every volume of space above the surface of the object. This is determined by the local velocity. Ignoring loss processes and outside forces, the densities of the bound,  $n_b(r)$ , and escaping,  $n_{es}(r)$ , components for a spherically symmetric atmosphere are readily calculated using the radial velocity,  $dr/dt$  [Johnson, 1990]:

$$n_b(r) = \Phi(1 - f_{es}) < 2(R_S/r)^2 / (dr/dt) >_b;$$

$$n_{es}(r) = \Phi f_{es} < (R_S/r)^2 / (dr/dt) >_{es}$$

where  $\Phi$  is the surface flux and  $R_S$  the satellite radius. The brackets imply averaging over the bound and escaping trajectories respectively, which can be carried out analytically for a number of characteristic energy distributions [Johnson, 1990]. If the flux is non-uniform and the transport distances are not large then such expressions can be used locally. If escape is negligible, then the atmosphere is locally flat. For thermal desorption this gives a density vs. altitude like the barometric law

$$n_j(z) = [N_j / H_j] \exp(-z/H_j);$$

$$N_j = \Phi_j [2\pi H_j/g]^{1/2}$$

with  $N_j$  the column density. Observers tend to interpret their data with such expressions even when the ejection process is not Maxwellian. Using the sputter energy distribution above for a locally flat atmosphere, then  $n_j(z) = [N_j / 2H_j^c][1 + z/H_j^c]^{-3/2}$ ;  $N_j = \Phi_j \pi (2U_j/M_j)^{1/2} / g$ ;  $H_j^c = U_j/M_j g$ , where  $H_j^c$  is like a 'scale' height and  $\Phi_j = Y_j \phi$  with  $Y_j$  the sputter yield.

When particles hop across the surface with full accommodation, the density can vary roughly as  $n \propto T^{-5/2}$  exhibiting a minimum at the subsolar point [Hodges and Johnson, 1968]. The lunar He atmosphere roughly exhibits such a trend [Hodges et al., 1974], but the lack of accommodation modifies the distribution [Shemansky and Broadfoot, 1977]. Lunar Ar also exhibits daily transients. Because it adsorbs at the nighttime temperatures there is a maxima near sunrise due to desorption and flow across the terminator with a smaller maximum at sunset [Hodges, 1980a]. Sodium is likely depleted in

the Mercury's subsolar regions, accumulating at higher latitudes where it is ejected by a stimulated desorption process. In contrast, the lunar alkali peak at the subsolar point.

Expressions can be created for non-isotropic atmospheres, but typically Monte Carlo simulations are carried out. The particles are launched from the surface using a choice of energy and angle determined from the ejecta distribution,  $f(E, \theta)$ . The space around the body is divided into volumes and the ejected particles are tracked in their ballistic trajectories noting the time,  $\Delta t$ , spent in each volume. A large number of particles are ejected and the average density is calculated from the sum of the  $\Delta t$  for all of the particles passing through a box times a surface flux,  $\Phi_j$ , divided by the radial extent of the box and the number of simulation particles [Bird, 1994]. If the ionization times are comparable to the flight times, then in each box the loss probability,  $\Delta P_L$ , is calculated and interaction with the solar radiation can be included. Monte Carlo models have been used to describe Ar and He at the moon [Hodges, 1980b] and the net transport of water molecules across the surface of Europa and Ganymede [Sieveka and Johnson, 1982]. More recently, they were used to describe the sodium component at Europa [Leblanc et al., 2001] and at Mercury and the Moon [Smyth and Marconi, 1995a, b].

### 3. ATMOSPHERES

#### 3.1. Mercury

Hydrogen, helium and probably oxygen were discovered by the Mariner spacecraft, but only upper limits were obtained for rare gases other than He. The H and He atmospheres are primarily due to the implantation of solar wind ions with radioisotope decay from uranium and thorium contributing He. The implantation flux is controlled by the variable interaction of the solar wind ions and fields with Mercury's magnetic field. The He distribution is roughly characterized by the surface temperature and exhibits a nighttime maximum [Hodges et al., 1973]. The H atmosphere has a quasi-thermal ( $\sim 400\text{K}$ ) and a very cold ( $\sim 100\text{K}$ ) component which is not understood. Jeans escape is efficient at the dayside temperatures on Mercury. Atomic O, on the other hand, is likely a sputter product from a silicate [Walters et al., 1988] and the returning O readily reacts with the surface.

The discovery of the alkali atmospheres [Potter and Morgan, 1985, 1986] lead to the hope that remote sensing of the ambient gas could give information on the

surface composition. Although this has not been realized, considerable interest was generated in atmospheric models. Solar wind sputtering [Potter and Morgan, 1985] and micrometeorite vaporization [Morgan et al., 1988, 1989; Hunten and Sprague, 1997] were initially suggested as the source of the alkalis. The solar wind ion sputtering source was found to be too small, and photon-stimulated desorption and thermal desorption were suggested to be important [Ip, 1986; McGrath et al., 1986]. Ion sputtering can contribute an energetic tail to the ejecta and can cause enhanced diffusion of sodium to the surfaces of grains [McGrath et al., 1986]. Subsequently, solar ions were shown to have had greater access to Mercury's surface than assumed. The neutrals ionized and accelerated into the surface could be sputter agents [Cheng et al., 1987; Sarantos et al., 2001] and could lead to alkali transport and implantation [Sprague et al., 1997]. Chemical sputtering, in which the implanted hydrogen replaces alkalis, can also enhance sputtering [Potter, 1995] although the rates are not known. Finally, at equatorial temperatures thermal desorption is very efficient [Hunten and Sprague, 1997; Madey et al., 1998].

The suggestion that photon-stimulated desorption was important was based on rough estimates of  $\sigma_j^{des}$ . Yakshinskiy and Madey (1999) found that  $\sigma_j^{des}$  had a lower than expected threshold, was relatively large, and had a non-thermal ejecta distribution. Sodium adsorbs in relatively deep wells ( $>1\text{eV}$ ) [Yakshinskiy et al., 2000], so that replenishment of surface Na by either radiation-enhanced diffusion, by micrometeorite mixing, or by adsorption produces similarly bound Na, simplifying the modelling of thermal and stimulated desorption.

At present there is no consensus on the importance of the various 'non-thermal' processes, but a single process cannot account for the diverse set of observations [Sprague et al., 1997; Killen et al., 2001]. Understanding these observations is complicated by the spatial non-uniformity and temporal variability of the atmosphere [Sprague, 1992; Sprague et al., 1997]. These are caused by the daily surface temperature excursions, geologic features, variable solar activity and changes in Mercury's distance from the sun. However, suggestions of correlations with the solar EUV and radiation pressure were not seen in the largest single data set [Sprague et al., 1997]. It is likely that thermal desorption rapidly removes Na and K in the equatorial regions and photo-desorption becomes important at high latitudes. Morning-side enhancements have been reported [Sprague et al., 1997] but were not seen in other data

sets [Killen *et al.*, 1990, 2001]. Because the rotation rate is slow, observing such enhancements could be difficult. At high latitudes and on the nightside, precipitating ions can sputter the surface and pick-up alkali ions can be implanted, but the size of the region into which a significant flux of ions flows to the surface varies [Kabin *et al.*, 2000; Sarantos *et al.*, 2001]. Sprague *et al.* (1997) found little evidence for variations with solar activity, but Killen *et al.* (2001) find a 30% effect at high solar activity. They suggested that photo-desorption, ~70%, and micro-meteorite impact vaporization, ~30%, account for the observed sodium when the interaction with the solar fields is weak. Since photo-desorption is ineffective for many species but energetic ion sputtering is not, observers should look for new species at times of high solar activity such as the O observed by Mariner and the recent observation of Ca [Bida *et al.*, 2000].

Because the alkali loss rates are not negligible, replenishment is required. Energetic solar flare ions cause diffusion of sodium to the surface layers [McGrath *et al.*, 1986], meteoritic bombardment exposes fresh grains [McGrath *et al.*, 1986; Morgan *et al.*, 1989; Sprague, 1992; Hunten and Sprague, 1997] and delivers alkalis to Mercury [Morgan *et al.*, 1988; Cintila, 1992]. Replenishment can also be affected by the differences in the age and properties of the surface [Sprague, 1990; Sprague *et al.*, 1998].

### 3.2. The Moon

The Moon's noble gas atmosphere was studied during the Apollo program. A weak upper limit to the total atmospheric density of  $2 \times 10^7/\text{cm}^3$  and a nighttime surface density  $\sim 10^2$  to  $2 \times 10^5/\text{cm}^3$  were obtained within about a factor of 2. These observations are both consistent with a surface boundary layer atmosphere. The rough upper limits, however, are larger than the maximum in the primary species observed,  $\sim 5 \times 10^4/\text{cm}^3$  each for He and Ar, suggesting other components are present. The Ar atmosphere, primarily  $^{40}\text{Ar}$  derived from radiogenic decay of  $^{40}\text{K}$  [Hodges, 1977] with ~10% from solar  $^{36}\text{Ar}$ , showed a daily transient which, because it is cold-trapped at night ( $\sim 100\text{K}$ ), exhibits maxima a large maximum at sunrise and a small maximum at sunset. For an ionization lifetime,  $\tau_i$ , of ~25 days Ar is lost in ~50 days with ~80% of the time spent adsorbed [Hodges, 2001]. The release rate from the interior also appears to be variable, possibly due to tidal stress. Helium does not condense at night and shows an inverse correlation with surface temperature. It is primarily supplied by the solar wind with ~10% radio-

genic component. Implanted He is removed from the regolith primarily by sputter erosion [Hodges and Hoffman, 1974]. Loss is due to Jeans escape with a small fraction lost by a non-thermal process.  $^{222}\text{Rn}$  and  $^{210}\text{Po}$  were observed through  $\alpha$  decay. The large difference in emission rates and the much shorter half life was evidence for episodic venting of Rn near to the time of observation and their spatial distribution correlated with surface features [Gorenstein *et al.*, 1974]. Other elements are now being mapped using Lunar Prospector data [Feldman *et al.*, 1998b]. Finally, an unconfirmed, but suggestive, detection of masses 15-16, 28 and 44 was made by Apollo [Hodges *et al.*, 1974].

The initial ground-based observations of the sodium and potassium atmosphere at the Moon [Potter and Morgan, 1988] were followed by a large number of observation of the local [e.g., Sprague *et al.*, 1996] and distant (escaping) atmosphere [Mendillo *et al.*, 1997b, Mendillo *et al.*, 1999]. Recently, Smith *et al.* (1998) observed a pulse of sodium from the Moon seen down stream due to the solar radiation pressure and focused by the earth's gravitational field. This pulse was associated with the Leonid meteorite shower [Hunten *et al.*, 1998], confirming that meteoritic impact vaporization contributes [Hunten *et al.*, 1991]. The sodium escape increased by a factor of 2-3 during the shower [Wilson *et al.*, 1999], but the atmospheric geometry suggests that meteorite bombardment is not the dominant steady state source of sodium.

The alkali atmosphere is only  $\sim 10^{-3}$  of the Ar and He atmospheres with average near surface densities of  $\sim 1-15 \text{ Na}/\text{cm}^3$  and maximum subsolar density  $\sim 30-70 \text{ Na}/\text{cm}^3$ . Because the Moon does not have a global field, and because the surface temperatures are lower and the radiation pressure is smaller, the alkalis at the Moon are simpler to describe than at Mercury. Since the Moon is less massive and the excursion distances are larger, escape is more important and a large, nearly global atmosphere peaked at the subsolar point results [Sprague *et al.*, 1996; Potter and Morgan, 1997] as indicated in the image in Plate 1 [Flynn and Mendillo, 1993]. Unlike lunar Ar, thermal desorption and transport of alkalis is only possible close to the subsolar point [Kozlowski *et al.*, 1990; Madey *et al.*, 1998]. As at Mercury there has been disagreement on the dominant desorption process. Observations of the line profile indicate that the atmosphere has a non-thermal component ( $\sim 1500\text{K}$ ) [Stern *et al.*, 2000]. The scale height increases with increasing zenith angle and can be fit by a thermal and non-thermal process [Stern and Flynn, 1995; Sprague *et al.*, 1996]. Recent laboratory measurements for photo-

stimulated desorption and the observations during the meteor shower confirm that these processes contribute.

*Mendillo et al.* (1999) noted the distant atmosphere did not change by large amounts when the Moon is in the Earth's magnetotail, but *Potter et al.* (2000) saw variations when the Moon passed through the magnetotail. They concluded that solar particle bombardment affects the supply of Na and K to the surface layers of grains. This occurs by enhanced diffusion due to energetic ion bombardment [*McGrath et al.*, 1986]. Except possible near the subsolar point, the surface species are primarily ejected by photo-desorption [*Sprague et al.*, 1996] with  $\sim 15\%$  by micrometeorites [*Mendillo et al.*, 1999]. Photo-desorption was shown to be sufficiently robust and the average ejecta speed can account for the cloud morphology [*Yakshinskiy and Madey*, 1999]. Desorption cross sections averaged over the solar spectrum are needed to convert the surface source rates into surface concentrations.

The alkali atmospheres peak more sharply than a cosine of the zenith angle [*Mendillo et al.*, 1997b; *Potter and Morgan*, 1999], due either to a contribution from thermal desorption, a temperature dependence in the photo-desorption rate or due to the product of a supply rate (sputter-enhanced diffusion) and a desorption rate both dependent on cosine of the zenith angle. *Sprague et al.* (1996) suggested a model in which stimulated desorption is followed by thermal hopping. As discussed, the recently measured adsorption energies are somewhat larger than the ones they used.

The line-of-site brightness of the sodium atmosphere over the limb decays as  $\sim R^{-4}$  at half moon and  $\sim R^{-2}$  at full moon [*Mendillo et al.*, 1993], where  $R$  is distance to the moon. These indicate the atmosphere has a gravitationally bound component and an extended non-thermal component as discussed. At large distances ( $>4R_M$ ) it decays more slowly, consistent with an escaping component [*Mendillo et al.*, 1997a, b, 1999]. There is, however, unexplained variability [*Hunten et al.*, 1991] possibly due to meteorites or charging of the lunar grains, particularly near the terminator. Charging depends on the solar wind conditions and can affect alkali transport within the grains and cause levitation/exposure of grains [*Zook and McCoy*, 1991; *Manka and Michel*, 1971].

The constraints on the total atmosphere from Apollo and detection of additional masses by one Apollo instrument suggest there are additional species, but only upper limits have been obtained [*Flynn and Stern*, 1996]. Since thermal and photo-desorption appear to dominate most of the time, this places severe constraints on

the ejection of other species. That is, a species must not only be more abundant than Na but also 'volatile'. However, when solar particles or micrometeorites cause ejection, additional species *should be seen*. The observed lunar pick-up ions  $O^+$ ,  $Al^+$  and  $Si^+$  [*Mall et al.*, 1998], which have masses close to those seen by Apollo, are suggestive of an energetic ejection process. Some oxygen is always produced on sputtering of a silicate [*Walters et al.*, 1988] and oxygen is released during the formation of the iron coatings on lunar grains [*Hapke*, 2001]. Since H was not seen at levels suggested, implanted H can reduce the surface releasing oxidants which may be molecular. Since detecting even trace species is important, this might be best done by in-situ measurement of the local pick-up ions [*Manka and Michel*, 1973; *Johnson and Baragiola*, 1991].

### 3.3. Galilean Satellites

Although Io's atmospheric density is controlled by its interaction with the surface, it has a collisionally thick atmosphere, except, possibly, at the poles and on the nightside. It is also an atmosphere for which escape is important, hence it is discussed in II.2 and III.4. Jupiter's large icy satellites, on the other hand, appear to have global surface boundary layer atmospheres. These atmospheres are formed by radiation-induced decomposition of surface materials, sputtering and thermal desorption. To date,  $O_2$ , Na, K and possibly hydrogen have been observed at Europa and oxygen and hydrogen have been identified at Ganymede. At Callisto atmospheric  $CO_2$  has been identified. In addition, ionospheres were observed by *Kliore et al.* (1997) on all three satellites.

These moons experience differences in tidal heating, affecting their geological evolution, and differences in the radiation flux to the surface, which increases by two to three orders of magnitude in going from Callisto to Europa [*Cooper et al.*, 2001]. Therefore, the surface age decreases from Callisto to Europa. These moons are all thought to have subsurface oceans [e.g., *Khurana et al.*, 1998]. The depth below the surface is probably the smallest at Europa, accounting for its apparent resurfacing. At Callisto primordial  $CO_2$  may be outgassing [*Carlson*, 1999].

Impacts and radiation bombardment produce brightening of the surface in competition with thermal annealing [*Johnson*, 1997]. Micrometeorites mix the surface, primarily on the hemisphere leading the satellite's motion, and may be responsible for the accumulated dark material on Callisto. Since the principal condensed volatile is  $H_2O$  the atmospheres are assumed to have

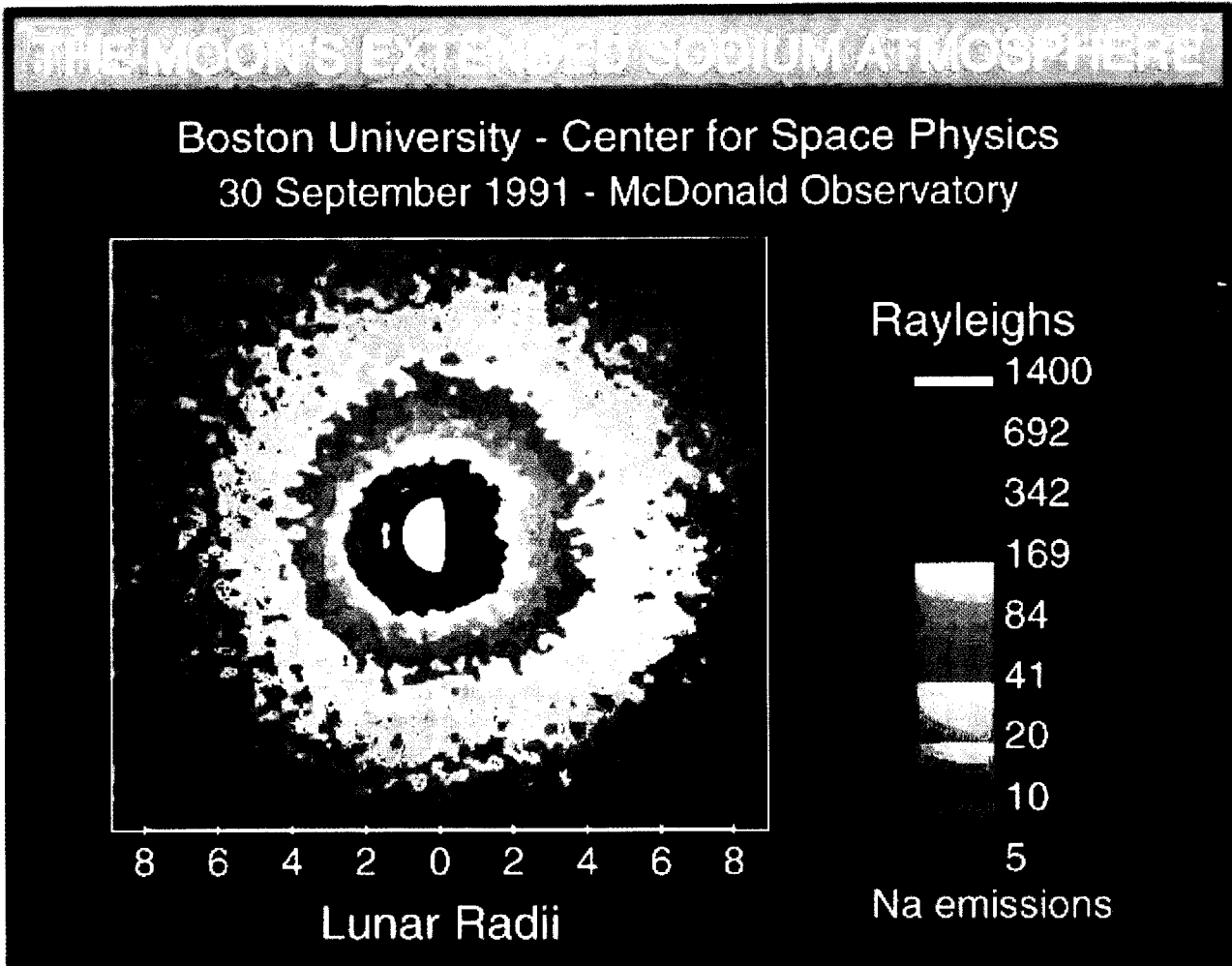


Plate 1. An image of the distant lunar atmosphere. This indicates that the maximum is roughly at the subsolar point [Flynn and Mendillo, 1993].

water vapor produced by sublimation in the equatorial regions and by sputtering elsewhere. The H<sub>2</sub>O column density is controlled by condensation on the nightside and at high latitudes. Other atmospheric species are produced by radiolysis. Whereas H<sub>2</sub>O adsorbs when it returns to the surface, the H<sub>2</sub> and O<sub>2</sub> produced by decomposition of ice do not. The H<sub>2</sub> predominantly escapes but the O<sub>2</sub> remains and becomes the dominant gas at Europa. The loss of hydrogen produces an oxidizing surface [Johnson and Quickenden, 1997], which has been suggested as a potential energy source for biology [Chyba, 2000; Cooper et al., 2001]. O<sub>2</sub> molecules that do not directly escape thermally desorb on each return to the surface until they are eventually dissociated or ionized. Therefore, the O<sub>2</sub> atmosphere will have a two component velocity distribution [Ip, 1996; Shematovich and Johnson, 2001], a large thermally accommodated component and a more energetic directly ejected component [Johnson, 1990]. Because the incident plasma determines both the source and loss processes, large column densities do not accumulate. Assuming electron impact ionization is the dominant loss process, a column of  $\sim 3 \times 10^{15}$  O<sub>2</sub>/cm<sup>2</sup> was predicted [Johnson et al., 1982; Johnson, 1990] in equilibrium with a larger column of O<sub>2</sub> in the regolith.

Hall et al. (1998) detected the excited O produced by dissociation of O<sub>2</sub>. They estimated a column density  $\sim 10^{15}$ /cm<sup>2</sup>. Subsequent modeling by Saur et al. (1998) suggested  $\sim 6 \times 10^{14}$  /cm<sup>2</sup> due to efficient loss by knock-on collisions. Recently [Shematovich and Johnson, 2001], ionization was found to be dominant, as initially suggested, and a larger than predicted source rate for O<sub>2</sub> was needed. A large source may be due to radiolysis by energetic electrons, the dominant energy source to the surface of Europa [Paranicas et al., 2001], to ionized re-impacting oxygen [Ip, 1996] or to over correcting for regolith structure. Photolysis of gas-phase H<sub>2</sub>O might also contribute. A global distribution of O<sub>2</sub> is usually assumed in modelling even though the non-ice materials dominate the equatorial regions on Europa's trailing hemisphere. However, recent HST images suggest that the O<sub>2</sub> atmosphere is localized around the icy regions [McGrath et al., 2000].

The Na and K observed on Europa come from decomposition and sputtering of surface materials [Johnson, 2001], presumably hydrated salts from the putative subsurface oceans [Kargel, 1991; McCord et al., 1998; Zolotov and Shock, 2001]. Although knock-on sputtering occurs, electronic sputtering is the dominant ejection process. The Na ejected from a hydrated salt is replaced by H forming frozen hydrated sulfuric acid,

which is suggested to be present by the IR spectra from the NIMS instrument on Galileo [Carlson et al., 1999a].

A Monte Carlo simulation of the morphology of the Na atmosphere was used to estimate a spatial and speed distribution of the ejected Na. Jupiter is the dominant perturbation as seen in the contour plot of the Na density distribution in Figure 2. Loss is due to Jeans escape and ionization but most ( $\sim 70\%$ ) of the electronically sputtered Na and K return to the surface [Johnson et al., 2001]. Since the average angular excursion is  $\sim 60^\circ$ , the Na is redistributed across Europa. The cloud morphology is found to be better reproduced by the measured energy distribution for electronic sputtering of Na adsorbed on ice [Johnson et al., 2001] than that for Na sputtered from a salt, Na<sub>2</sub>SO<sub>4</sub> [Wiens et al., 1997]. This indicates that most of the ejected sodium was adsorbed in ice-rich materials [Johnson, 2000]. There is likely a tail corresponding to sputtering from more refractory materials, but the distant Na observations show considerable variability, probably due Europa's interaction with the jovian magnetosphere [Leblanc et al., 2001]. The measured energy distributions were used to convert the observed Na/K ratio [Brown and Hill, 1996] into a relative surface source strength, Na/ K  $\sim 20$ , and relative total loss rate Na / K  $\sim 27$  [Johnson et al., 2001]. Since the desorption cross sections are similar, the surface region is rich in Na relative to K as compared to models of the putative subsurface ocean (Na/K  $\sim 14$ -19). This is consistent with fractionation during upwelling and freezing [Zolotov and Shock, 2001]. The Na concentration in the optical layer is  $\sim 0.01$ - $0.005$  with the atmospheric surface densities at the apex of the trailing hemisphere  $\sim 300$  Na/cm<sup>3</sup> and 15 K/cm<sup>3</sup>.

Other species should be detectable at Europa. SO<sub>2</sub>, seen in the irradiated dark regions, is produced radiolytically and by implantation. These regions obtain their reddened spectra due to radiolytic production of chain sulfur [Johnson et al., 1988]. In Io's polar regions radiolysis of SO<sub>2</sub> produces sulfur [Johnson, 1997], but in the presence of ice radiolysis of sulfur gives the three detected forms: primarily H<sub>2</sub>SO<sub>4</sub>. XH<sub>2</sub>O, with much smaller ( $\sim 1\%$ ) amounts of SO<sub>2</sub> and S<sub>x</sub> in ice and very small amounts of H<sub>2</sub>S [Carlson et al., 1999a; Carlson et al., 2001]. The sulfur could be implanted by the bombarding plasma [Lane et al., 1982], due to venting as at Io, or a sulfate from the subsurface ocean [Johnson, 2001]. The S<sub>x</sub>, which darkens the surface, can be slowly removed by oxidation to SO<sub>2</sub> and sputtering. Therefore, a fresh sulfur containing surface, which is rapidly darkened radiolytically, can 'brighten' over long periods of time [Carlson et al., 2001].

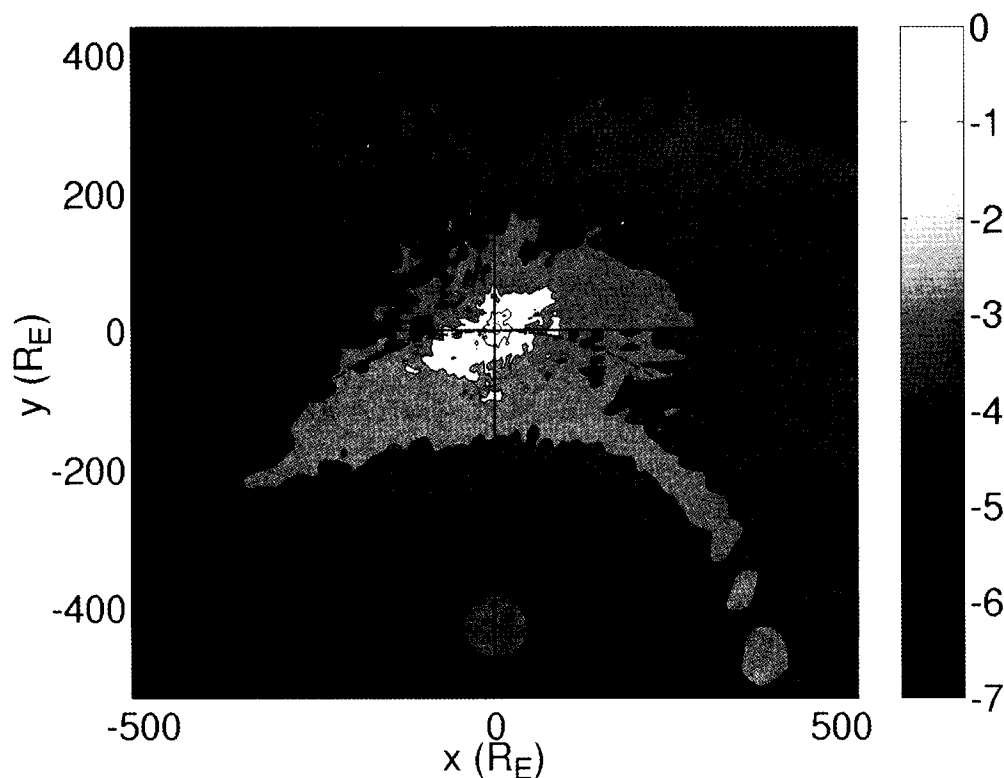


**Figure 2.** The calculated density of the distant sodium atmosphere at Europa cut along the Europa orbital plane. Jupiter is represented by the circle on the axis  $x=0$ . Grey levels correspond to density varying by factors of  $10^{-1}$  from  $\sim 1 \text{ Na cm}^{-3}$  close to Europa, to  $10^{-7} \text{ Na cm}^{-3}$ , far from Europa ignoring contributions from Io. [Johnson *et al.*, 2001].

Ganymede is presumed to be similar to Europa, but its surface is older and, as at Callisto,  $\text{CO}_2$  is seen trapped in ice [Hibbitts *et al.*, 2000]. It also has an intrinsic magnetic field large enough to shield regions of the surface from the plasma flow. The flow and magnetic pressure are variable due to Jupiter's tilted dipole and 'turbulence' within the trapped plasma. Particle precipitation primarily occurs onto Ganymede's high latitudes ( $> \sim 40^\circ$ ). Frost growth by vapor deposition and radiation damage can produce the bright, unannealed polar regions [Johnson, 1997] and radiolysis produces an  $\text{O}_2$  polar atmosphere, resulting in an aurora (see I.4) and an  $\text{O}_2^+$  ionosphere [Eviatar *et al.*, 2001]. At low latitudes, where atmospheric O has been seen [Brown *et al.*, 1999], a collisional subsolar atmosphere can exist *if* the surface is predominantly ice, in which case  $\text{O}_2$  might also be formed by gas-phase photolysis [Kumar and Hunten, 1982].  $\text{O}_2$ , probably trapped in Ganymede's icy surface, is seen at mid to low latitudes [Calvin *et al.*, 1996] where photon path lengths in the surface are relatively long [Johnson and Jessor, 1997]. Alternatively, a large  $\text{O}_2$  atmosphere or frozen patches

of  $\text{O}_2$  have been suggested [Vidal *et al.*, 1997]. The amount of 'trapped'  $\text{O}_2$  seen at Europa is an order of magnitude smaller than that at Ganymede [Spencer and Klesman, 2001] due either to chemical competition with sulfur or the short photon path-length in its bright surface. The  $\text{O}_2$  produced at depth by the most penetrating particles can slowly diffuse to the surface. An  $\text{O}_3$ -like feature is seen at higher latitudes [Noll *et al.*, 1996; Hendrix *et al.*, 1999], which is likely to be a trapped species produced from  $\text{O}_2$ . Hydrated minerals and trace amounts of  $\text{SO}_2$  and  $\text{CO}_2$  are also seen [McCord *et al.*, 1998]. Trapped volatiles, can be released by meteorite impacts or by enhanced-diffusion and sputtering by energetic charged particles.

Callisto's surface is heavily cratered and much older. The crater morphology suggests that the surface is weathered, possibly by desiccation or by long term energetic particle radiation. Atmospheric  $\text{CO}_2$  has been seen by the NIMS instrument on Galileo at a column density  $\sim 10^{14}/\text{cm}^2$  [Carlson, 1999] and in the surface ices [Hibbitts *et al.*, 2000]. Whereas the surface appears covered in a lag deposit, water ice is associated with

'fresh' impact features. The atmospheric CO<sub>2</sub> has been suggested to be due to slow outgassing, but may be a radiation-induced decomposition product of a carbonate or organic molecules in the surface [Johnson, 2001].

### 3.4. Saturnian Satellites and Rings

The small icy satellites of Saturn have low escape energies and very tenuous atmospheres consistent with ice at <~100K. The atmospheres are dominated by escape and the vapor pressure is low, so sputtering and particulate impacts are important sources. Consistent with radiation-induced decomposition, the reddening in the UV is suggestive of H<sub>2</sub>O<sub>2</sub> and O<sub>3</sub> [Noll *et al.*, 1997] present in the surface. Therefore, H<sub>2</sub>O, O<sub>2</sub> and H<sub>2</sub> are likely the dominant ejecta with smaller amounts of radicals [Kimmel *et al.*, 1995]. Based on the expected velocity distributions, the escape fractions are ~0.9, 0.8, 1, respectively at Dione [Johnson, 1990]. None of these molecules have been seen as gravitationally bound species, but their presence is inferred from the ambient OH and H [Richardson *et al.*, 1998]. That is, the escaping molecules have long (~yr.) lifetimes in orbit about Saturn. A H cloud [Shemansky and Hall, 1992] and a toroidal OH cloud were observed [Shemansky *et al.*, 1993]. The latter occupies the region in which the icy satellites and Saturn's E-ring particles orbit. A small fraction of H and OH is derived by sputtering of the icy satellites [Jurac *et al.*, 2001b]. Other volatiles should be seen, like the CO<sub>2</sub> or SO<sub>2</sub> seen at the Jovian satellites or nitrogen and ammonia from an ammonia hydrate.

Analysis of the OH cloud [Jurac *et al.*, 2001a] showed that a large source is missing in the vicinity of Enceladus. Therefore, more icy surface area must be present in this region, possibly produced by small colliding icy objects, or the icy surfaces contain volatiles which would make sputtering more efficient. An active Enceladus has also been suggested because of its bright surface and because the E-ring peaks near its orbit [Stevenson, 1982]. The surfaces of the icy satellites and objects in the main rings are bombarded by both micrometeorites [Haff and Eviatar, 1986; Pospieszalska and Johnson, 1991] and by charged E-ring grains in eccentric orbits [Hamilton and Burns, 1994]. These processes can produce additional water vapor, but their net effect is not well established. This is due both to the absence of data on the impacting fluxes and a lack of knowledge of the vapor production efficiency from a porous icy surface. The distant icy moons of Saturn, such as Iapetus, have surface features that also suggest weathering processes are occurring. The principal atmospheric sources are likely solar wind sputtering and photodesorption.

### 3.5. Other Bodies

The icy moons of Uranus also exist in a trapped magnetospheric plasma. However, the plasma density is small because of the unusual orientation of the magnetic field to the satellite's orbital motion. Since the plasma is primarily protons from the atmosphere of Uranus, sputtering is less robust and but radiolysis occurs. Based on their reflectance, these satellites apparently experienced radiation darkening due to a carbon containing molecule in the ice [Lanzerotti *et al.*, 1987; Strazzulla, 1998].

When Pluto is inside the orbit of Neptune it has a significant atmosphere which is similar to Triton's. These atmospheres are primarily N<sub>2</sub> with a few percent CH<sub>4</sub> and CO. Pluto's surface is roughly in local vapor pressure equilibrium [Trafton, 1990]. In its present position the atmosphere is collisional. Charon, on the other hand, has a surface which is predominantly ice with a contaminant like that seen on other icy moons, possibly an ammonia hydrate or trapped CO<sub>2</sub>, but shows no evidence of the volatiles found on Pluto and Triton [Buie and Grundy, 2000]. With a disc-averaged surface temperature of ~60K, solar wind sputtering and photodesorption are likely principal contributors to Charon's atmosphere. If the suggested hydrated ammonia exists on the surface, the atmosphere will contain N<sub>2</sub> as a decomposition product [Johnson, 1998]. Because of decomposition, the hydrate is removed preferentially, so the subsurface concentration is likely larger than that at surface.

Although they are not surface boundary layer atmospheres, the atmospheres of Triton and Pluto exhibit interesting interactions with their surfaces (see III.4). Nitrogen ice is in vapor pressure equilibrium with the N<sub>2</sub> atmosphere. Since N<sub>2</sub> is more strongly absorbing in the thermal IR than in the visible, sunlight is absorbed at greater depths than that depth from which thermal emission occurs producing a solid state greenhouse effect. This causes sublimation at depth into the regolith with condensation near the surface [Grundy and Stansberry, 2000]. Since CH<sub>4</sub> is much less volatile, it is seen at higher concentrations in the surface than in the atmosphere, possibly concentrated by the greenhouse effect. This effect may also seal off the surface allowing the formation of the observed geysers.

## 4. SUMMARY

In this chapter I have summarized our understanding of surface boundary atmospheres on a number of solar system bodies. I have also very briefly described the physical processes controlling their composition and

density. These atmospheres are interesting for two reasons. By monitoring such atmospheres we can learn about the external weathering agents. But what is more exciting, because of the paucity of spacecraft missions to distant objects, remote sensing of these atmospheres can lead to information on their surface composition. Understanding of the weathering processes and composition can lead, in principal, to an understanding of the evolution of these bodies. To make this a reality, an enhanced observing effort must be accompanied by an enhanced laboratory / modeling effort to study the relevant desorption processes.

*Acknowledgments.* The author would like to thank the M. Combi, R. Hodges, D. Hunten, M. Mendillo and A. Sprague for comments and suggestions. This work was supported by NASA's Planetary Atmospheres Program.

## REFERENCES

- Bahr, D.A., M.A. Fama, R.A. Vidal, and R.A. Baragiola, Radiolysis of water ice in the outer solar system: Sputtering and trapping of radiation products, *J. Geophys. Res.* in press 2001.
- Bida, T.A., R.M. Killen, T.H. Morgan, Discovery of calcium in Mercury's atmosphere, *Nature* 404, 159-161, 2000.
- Bird, G.A., Molecular Gas Dynamics and Direct Simulation of Gas Flows, Clarendon, Oxford, England 1994.
- Brown, M.E., R.E. Hill, Discovery of an extended sodium atmosphere around Europa, *Nature* 380, 229-231, 1996.
- Brown, M.E., Potassium in Europa's atmosphere, *Icarus* 151, 190-195, 2001.
- Brown, M.E., A.H. Bouchez, Observations of Ganymede's Visible Aurorae, *BAAS, DPS Meeting #31, #70.08*, 1999.
- Brown, R.A., F.H. Chaffee Jr, High resolution spectra of sodium emission from Io, *Astrophys. J.* 187, L125-L126, 1974.
- Buie, M.W. and W.M. Grundy, The Distribution and physical state of H<sub>2</sub>O on Charon, *Icarus* 148, 324-339, 2000.
- Calvin, W. M., R. E. Johnson, and J. A. Spencer, O<sub>2</sub> on Ganymede: Spectral characteristics and plasma formation mechanisms, *Geophys. Res. Lett.* 23, 673-676, 1996.
- Carlson, R.W., A Tenuous carbon Dioxide Atmosphere on Jupiter's Moon Callisto, *Science* 283, 820-821, 1999.
- Carlson, R.W., R.E. Johnson, and M.S. Anderson, Sulfuric acid on Europa and the radiolytic sulfur cycle, *Science* 286, 97-99, 1999a.
- Carlson, R.W., +13 authors, Hydrogen peroxide on the surface of Europa, *Science* 283, 2062-2064, 1999b.
- Carlson, R.W., M.S. Anderson, and R.E. Johnson, Sulfuric acid production on Europa: The radiolysis of sulfur in water ice, *Icarus* submitted, 2001.
- Cheng, A.F. and L.J. Lanzerotti, Ice sputtering by radiation belt protons and rings of Saturn and Uranus, *J. Geophys. Res.* 83, 2597-2602, 1978.
- Cheng, A.F., R.E. Johnson, L.J. Lanzerotti, and S.M. Krimigis, Magnetosphere exosphere, and surface of mercury, *Icarus* 71, 430-440, 1987.
- Chyba, F., Energy for Microbial life on Europa, *Nature* 403, 381-382, 2000.
- Cintila, M.J., Impact-induced thermal effects in the lunar and Mercurian regoliths, *J. Geophys. Res.* 97, 947-973, 1992.
- Cooper, J.H., R.E. Johnson, B.H. Mauk, H.B. Garrett, and N. Gehrels, Energetic ion and electron irradiation of the icy galilean satellites, *Icarus* 149, 133-159, 2001.
- Eviatar, A., V. Vasyliunas, and D. Gurnett, The ionosphere of Ganymede. *Planet. Planet. Space Sci.* 49, 327-336, 2001.
- Feldman, W.C., S. Maurice, A.B. Binder, B.L. Barraclough, R.C. Elphic, and D.J. Lawrence, Fluxes of fast and epithermal neutrons from Lunar Prospector: Evidence for water ice at the poles, *Science* 281, 5382, 1998a.
- Feldman, W.C., B.L. Barraclough, S. Maurice, R.C. Elphic, D.J. Lawrence, D.R. Thomsen, and A.B. Binder, Major compositional units of the Moon: Lunar Prospector: data, *Science* 281, 1489-1493, 1998b.
- Flynn, B. and M. Mendillo, A picture of the Moon's atmosphere, *Science* 261, 184-186, 1993.
- Flynn, B. and S.A. Stern, A spectroscopic survey of metallic species abundances in the lunar atmosphere, *Icarus* 124, 530-536, 1996.
- Goldstein, B.E., S.T. Suess, and R.J. Walker, Mercury: Magnetospheric processes and the atmospheric supply and loss rates, *J. Geophys. Res.* 86, 5485-5499, 1981.
- Grundy, W.M. and J.A. Stansberry, Solar gardening and the seasonal evolution of nitrogen ice on Triton and Pluto, *Icarus* 148, 340-346, 2000.
- Gorenstein, P., L. Golub, and P.L. Bjorkholm, Detection of radon emission at the edges of lunar maria with the Apollo alpha-particle spectrometer, *Science* 183, 411-413, 1974.
- Haff, P.K. and A. Eviatar, Micrometeoroid impact on planetary satellites as a magnetospheric mass source, *Icarus* 66, 258-269, 1986.
- Hall, D.T., P.D. Feldman, M.A. McGrath, and D.F. Strobel, The far-ultraviolet oxygen airglow of Europa and Ganymede, *Astrophys. J. Lett.* 499, 475-485, 1998.
- Hamilton, D. P. and J.A. Burns, Origin of Saturn's E Ring: Self-Sustained, Naturally, *Science* 264, 550-553, 1994.
- Hendrix, A.R., C.A. Barth and C.W. Hord, Ganymede's ozone-like absorber: observations by the Galileo ultraviolet spectrometer, *J. Geophys. Res.* 104(E6), 14169-14178, 1999.
- Hapke, B., On the sputter alteration of regoliths of the outer solar system bodies, *Icarus* 66, 270-279, 1986.
- Hapke, B., Space weathering from Mercury to the asteroid belt. *J. Geophys. Res.* 106, 10039-10073, 2001.
- Hibbitts, C.A., T.B. McCord, and G.B. Hansen, The distributions of CO<sub>2</sub> and SO<sub>2</sub> on the surface of Callisto, *J. Geophys. Res.-Planet.* 105, E9, 22541-22557, 2000.
- Hodges, R.R., Differential Equation of Exospheric Lateral Transport and Its Application to Terrestrial Hydrogen, *J. Geophys. Res.* 78, 7340-7346, 1973.
- Hodges, R.R., *PEPI* 14, 282-288, 1977.
- Hodges, R.R., Lunar cold traps and their influence on Argon-40, *Proc. Lunar and Planet Sci. Conf.* 11, 2463-2477, 1980a.
- Hodges, R.R., Methods for Monte Carlo simulation of the exospheres of the Moon and Mercury, *J. Geophys. Res.* 85, 164-170, 1980b.
- Hodges, R.R., Ice in the lunar polar regions revisited, *Icarus*, in press 2001.

- Hodges, R.R. and Hoffman, *Geophys. Res. Letts.* 1, 69-71, 1974.
- Hodges, R.R. and F.S. Johnson, *J. Geophys. Res.* 73, 7307-7317, 1986.
- Hodges, R.R., J.H. Hoffman, and F.S. Johnson, Composition and dynamics of the lunar atmosphere, *Geochimica et Cosmo. Acta.* 3, (Suppl. 4) 2855-2864, 1973.
- Hodges, J.H. Hoffman, and F.S. Johnson, The lunar atmosphere, *Icarus* 21, 415-440, 1974.
- Huebner, W.F., J.J. Keady, and S.P. Lyon, Solar photo-rates for planetary atmospheres and atmospheric pollutants, *Astrophys. and Space Sci.* 195, 1-294, 1992.
- Hunten, D.M., T.H. Morgan, and D.E. Shemansky, The Mercury atmosphere, in *Mercury*, edited by F. Vilas, C.R. Chapman, and M.S. Matthews, pp.562-612, Univ. of Ariz. Press, Tucson, 1988.
- Hunten, D.M., The equilibrium of atmospheric sodium, *Planet. Space Sci.* 40, 1607-1614, 1991.
- Hunten, D.M., R.W.H. Kozlowski, and A.L. Sprague. A possible meteor shower on the Moon, *Geophys. Res. Lett.* 18, 2101-2104, 1991.
- Hunten, D.M. and A.L. Sprague, Origin and character of the Lunar and Mercurian atmospheres, *Adv. Space Res.* 19, 1551-1560, 1997.
- Hunten, D.M., G. Cremonese, A.L. Sprague, R.E. Hill, S. Vernai, and R.W.H. Kozlowski, The Leonid meteor shower and the Lunar sodium atmosphere, *Icarus* 136, 298-303, 1998.
- Ip, W.H., The sodium exosphere and magnetosphere of Mercury, *Geophys. Res. Lett.* 13(5), 423-426, 1986.
- Ip, W. -H. Europa's oxygen exosphere and its magnetospheric interaction, *Icarus* 120, 317-325, 1996.
- Johnson, R.E., Sputtering of a planetary regolith, *Icarus* 78, 206-210, 1989.
- Johnson, R.E., Energetic Charged-Particle Interactions with Atmospheres and Surface, *Springer-Verlag, Berlin* 1990.
- Johnson, R.E., Sputtering of ices in the outer solar system, *Rev. Mod. Phys.*, 68, 305-312, 1996.
- Johnson, R.E., Polar 'caps' on Ganymede and Io revisited, *Icarus* 128, 469-471, 1997.
- Johnson, R.E., Sputtering and desorption from icy surfaces, In *Solar System Ices* (B. Schmitt, C. deBergh Eds.) (Kluwer Netherlands, Dordrecht) pp.303-334, 1998.
- Johnson, R.E., Sodium at Europa, *Icarus* 143,429-433, 2000.
- Johnson, R.E., Surface chemistry in the Jovian magnetosphere radiation environment, In *Chemical Dynamics in Extreme Environments* (R. Dessler, Ed), *Adv. Ser. in Phys. Chem.* World Scientific, Singapore, Chapter 8, 390-419, 2001.
- Johnson, R.E. and E.C. Sittler, Sputter-produced plasma as a measure of satellite surface composition: The CASSINI mission, *Geophys. Res. Letts.* 17, 1629-1632, 1990.
- Johnson, R.E. and R.A. Baragiola, Lunar surface: Sputtering and secondary ion mass spectrometry, *Geophys. Res. Letts.* 18, 2169-2172, 1991.
- Johnson, R.E. and W. A. Jesser, Radiation-produced micro-atmospheres in the surface of Ganymede, *Astrophys. J. Lett.* 480, L79-L82, 1997.
- Johnson, R.E. and T.I. Quickenden, Photolysis and radiolysis of water ice on outer solar system bodies, *J. Geophys. Res.* 102, 10985-10996, 1997.
- Johnson, R.E., L.J. Lanzerotti, and W.L. Brown, Planetary application of ion induced erosion of condensed-gas frosts, *Nucl. Instrum. Methods* 198, 147-158, 1982.
- Johnson, R. E., M. Nelson, T.M. McCord, and J. Gradie, Voyager Images of Europa: Plasma Bombardment, *Icarus* 75, 423-436, 1988.
- Johnson, R.E., R.M. Killen, J.H. Waite Jr., and W.S. Lewis, Europa's surface composition and sputter-produced ionosphere, *Geophys. Res. Letts.* 25, 3257-3260, 1998.
- Johnson, R.E., F. Leblanc, B.V. Yakshinskiy, and T.E. Madey, Energy distributions for desorption of sodium and potassium from ice: the Na/K ratio at Europa, *Icarus*, in press 2001.
- Jurac, S., J.D. Richardson, M.A. McGrath, and V.M. Vasyliunas, A Eviatar. OH cloud in Saturn's magnetosphere, *BAAS, DPS meeting #32, #12.02*, 2000.
- Jurac, S., R.E. Johnson, and J.D. Richardson, Saturn's E-ring and production of a neutral torus, *Icarus* 149, 384-396, 2001a.
- Jurac, S., R.E. Johnson, J.D. Richardson, and C. Paranicas, "Satellite sputtering in Saturn's magnetosphere", *Planet Space Sci.* 49(3-4), 319-326, 2001b.
- Kabin, K., T.I. Gombosi, D.L. DeZeeuw, and K.G. Powell, Interaction of Mercury with the solar wind, *Icarus* 143, 397, 2000.
- Kargel, J.S., Brine volcanism and the interior structure of asteroids and icy satellites, *Icarus* 94, 368-390, 1991.
- Khurana, K.K., M.G. Kivelson, D.J. Stevenson, G. Schubert, C.T. Russell, R.J. Walker, and C. Polanskey, Induced magnetic fields as evidence for subsurface oceans in Europa and Callisto *Nature* 395, 777-780, 1998.
- Killen, R.M. and W.H. Ip, The surface-bounded atmospheres of Mercury and the Moon, *Rev. Geophys.* 37, 361-406, 1999.
- Killen, R.M., A.E. Potter, P. Reiff, M. Sarantos, B.V. Jockson, P. Hick, and B. Giles, Evidence for space weather at Mercury, *J. Geophys. Res.* 106, 20509-20525, 2001.
- Kimmel, G.A., T.M. Orlando, C. Vizina, and L. Sanche, Low energy electron-stimulated production of molecular hydrogen from amorphous water ice, *J. Chem. Phys.* 101, 3282-3286, 1994.
- Kimmel, G.A. and T.A. Orlando, Low-energy (5 - 120 eV) electron stimulated dissociation of amorphous D<sub>2</sub>O ice: D(<sup>2</sup>S), O(<sup>3</sup>P<sub>2,1,0</sub>), and O(<sup>1</sup>D) yields and velocity distributions, *Phys. Rev. Lett.* 75, 2606-2609, 1995.
- Kivelson, M.G., K.K. Khurana, C.T. Russell, R.J. Walker, J. Warnecke, F.V. Coroniti, C. Polanskey, D.J. Southwood, and G. Schubert, Discovery of Ganymede's magnetic field by the Galileo spacecraft, *Nature* 384, 537-541, 1996.
- Kliore, A., J.D.P. Hinson, F.M. Flasar, A.F. Nagis, and T.E. Crasens, The ionosphere of Europa from Galileo radio occultations, *Science* 277, 1239-1241, 1997.
- Kozlowski, R.W.H., A.L. Sprague, and D.M. Hunten, Observations of potassium in the tenuous lunar atmosphere, *Geophys. Res. Letts.* 17, 2253-2256, 1990.
- Kumar, S. and D.M. Hunten, The atmosphere of Io and other satellites, In *Satellites of Jupiter* (Ed.. D. Morrison) U of Arizona Press, Tucson pp782-806, 1982.
- Lane, A.L., R.M. Nelson, and D. L. Matson, Evidence for sulphur implantation in Europa's UV absorption band. *Nature* 292, 38-39, 1982.
- Lanzerotti, L.J., W.L. Brown, and K.J. Marcantonio, Experimental study of erosion methane ice by energetic ions and

- some consideration for astrophysics, *J. Astrophys.* 313, 910-919, 1987.
- Leblanc, F., R.E. Johnson, and M.E. Brown, Europa's sodium atmosphere: an ocean source? *Icarus* submitted 2001.
- Madey, T.E., B.V. Yakshinskiy, V.N. Ageev, R.E. Johnson, Desorption of alkali atoms and ions from oxide surfaces: Relevance to origins of Na and K in the atmospheres of Mercury and the Moon, *J. Geophys. Res.* 103, 5873-5888, 1998.
- Madey, T.E., R.E. Johnson, and T.M. Orlando, Far-out surface science: radiation-induced surface processes in the solar system, *Surface Science* in press 2001.
- Mall, U., E. Kirsch, K. Cierpka, B. Wilken, A. Soding, F. Neubauer, G. Gloeckler, and A. Galvin, Direct observation of lunar pick-up ions near the Moon, *Geophys. Res. Lett.* 25, 3799-3802, 1998.
- Manka, R.H. and F.C. Michel, Lunar atmosphere as a source of Argon-40 and other lunar elements, *Proc. Lunar Sci. Conf. 2nd, Geochimica Cosmochim Acta Suppl.* 2, 1717-1728, 1971.
- Manka, R.H. and F.C. Michel, Lunar ion flux and energy, In, Photon and Particle Interactions with surfaces in space (ed., R.J.L. Grard) (*D. Reidel, Dordrecht*) 429-442, 1973.
- Matsuura, T., Hot Atom Chemistry. Kodansha, Tokyo: *Elsevier, Amsterdam* 1984.
- McCord, T.B., +13 authors, Salts on Europa's surface detected by Galileo's near infrared mapping spectrometer, *Science* 280, 1242-1245, 1998.
- McGrath, M.A., R.E. Johnson, and L.J. Lanzerotti, Sputtering of sodium on the planet Mercury, *Nature* 22, 694-696, 1986.
- McGrath, M. A., P.D. Feldman, D.F. Strobel, K. Retherford, B. Wolven, and H.W. Moos, HST/STIS Ultraviolet imaging of Europa, *BAAS. DPS Meeting #32, #34.09*, 2000.
- Mendillo, M., B. Flynn, and J. Baumgardner, Imaging experiments to detect an extended sodium atmosphere on the Moon, *Adv. Space Res.* 13(10), 313-319, 1993.
- Mendillo, M., J. Wilson, J. Baumgardner, G. Cremonese, and C. Barbieri, Eclipse observations of the lunar atmosphere from the TNG site, in *The Three Galileos*, edited by J. Rahe et al. pp. 393-400, Kluwer Acad., Norwell, Mass., 1997a.
- Mendillo, M., J. Emery, and B. Flynn, Modeling the Moon's extended sodium cloud as a tool for investigating sources of transient atmosphere, *Adv. Space Res.* 19(3), 1577-1586, 1997b.
- Mendillo, M., J. Baumgardner, and J. Wilson, Observational Test for the Solar Wind Sputtering Origin of the Moon's Extended Sodium Atmosphere, *Icarus* 137, 13-23, 1999.
- Morgan, T.H., H.A. Zook, and A.E. Potter, Impact-driven supply of sodium and potassium to the atmosphere of Mercury, *Icarus* 75, 156-170, 1988.
- Morgan, T.H., H.A. Zook, and A.E. Potter, Production of sodium vapor from exposed regolith in the inner solar system, *Proc. Lunar Sci. Conf.* 19th, 297-304, 1989.
- Noll, K.S., R.E. Johnson, A.L. Lane, D.L. Dominigue, and H.A. Weaver, Detection of ozone on Ganymede, *Science* 273, 341-343, 1996.
- Noll, K.S., T. Roush, D. Cruikshank, R.E. Johnson, and Y.J. Pendleton, Ozone on Dione and Rhea, *Nature* 388, 45-47, 1997.
- Pappalardo, R.T., J.W. Head, and R. Greedy, The hidden ocean of Europa, *Scientific American*, Oct., 34-43, 1999.
- Paranicas, C., R.W. Carlson, and R.E. Johnson, Electron bombardment of Europa, *Geophys. Res. Lett.* 28, 673-676, 2001.
- Pospieszalska, M. and R.E. Johnson, Plasma ion bombardment profiles: Europa and Dione, *Icarus* 78, 1-13, 1989.
- Pospieszalska, M. and R.E. Johnson, Micrometeorite erosion of the main rings as a source of plasma in the inner Saturnian plasma torus, *Icarus* 93, 45-52, 1991.
- Potter, A.E., Chemical sputtering could produce sodium vapor and ice on Mercury, *Geophys. Res. Lett.* 22, 3289-3292, 1995.
- Potter, A.E. and T.H. Morgan, Discovery of sodium in the atmosphere of Mercury, *Science* 229, 651-653, 1985.
- Potter, A.E. and T.H. Morgan, Potassium in the atmosphere of Mercury, *Icarus* 67, 336-340, 1986.
- Potter, A.E. and T.H. Morgan, Discovery of sodium and potassium vapor in the atmosphere of Moon, *Science* 241, 657-680, 1988.
- Potter, A.E. and T. H. Morgan, Variation of the lunar solar emission with phase angle, *J. Geophys. Res.* 21, 2263-2266, 1994.
- Potter, A.E., R.M. Killen, and T.H. Morgan, Variation of lunar sodium during passage of the Moon through the Earth's magnetotail, *J. Geophys. Res.* 105, 15073-15084, 2000.
- Reimann, C.T., J.W. Boring, R.E. Johnson, J.W. Garrett, K.R. Farmer, and W.L. Brown, Ion-induced molecular ejection from D<sub>2</sub>O ice, *Surf. Sci.* 147, 227-240, 1984.
- Richardson, J.D., D.A. Eviatar, M.A. McGrath, and V.M. Vasyliunas. OH in Saturn's magnetosphere: Observation and implications, *J. Geophys. Res.* 103, 20245-20255, 1998.
- Roth, J., Chemical sputtering. In, *Sputtering by Particle Bombardment II*. Ed. R. Behrisch (*Springer Verlag, Berlin*) 91-141, 1983.
- Sarantos, B., P.H. Reiff, T.W. Hill, R.M. Killen, and A.L. Urquhart. A Bx-interconnected magnetosphere model for Mercury. *Planet. Space Sci.* in press 2001.
- Saur, J., D.F. Strobel, and F.M. Neubauer, Interaction of the Jovian magnetosphere with Europa: Constraints on the neutral atmosphere, *J. Geophys. Res.* 103, 19947-19962, 1998.
- Shemansky, D.E. and A.L. Broadfoot, Interaction of the surfaces of the Moon and Mercury with their exospheric atmospheres, *Rev. of Geophys. and Space Phys.* 15, 491-499, 1977.
- Shemansky, D.E. and D.T. Hall, The distribution of atomic hydrogen in the magnetosphere of Saturn, *J. Geophys. Res.* 97, 4143-4161, 1992.
- Shemansky, D.E., P. Matheson, D.T. Hall, H.-Y. Hu, and T.M. Tripp, Detection of the hydroxyl radical in the Saturn magnetosphere, *Nature* 363, 329-331, 1993.
- Shematovich, V.I. and R.E. Johnson, Near-surface oxygen atmosphere at Europa, *Adv. Space Res.* 27, 1881-1888, 2001.
- Shi, M., R.A. Baragiola, D.E. Grosjean, R.E. Johnson, S. Jurac, and J. Schou, Sputtering of water ice surfaces and

- the production of extended neutral atmospheres, *J. Geophys. Res.* 100, 26387-26395, 1995.
- Sieger, M.T., W.C. Simpson, T.M. Orlando, Production of O<sub>2</sub> on icy satellites by electronic excitation of low-temperature water ice, *Nature* 394, 554, 1998.
- Sieveka, E.M. and R.E. Johnson, Thermal - and plasma - induced molecular redistribution on the icy satellites, *Icarus* 51, 528-548, 1982.
- Smith, R.S. and B. D. Kay, Adsorption, desorption and crystallization kinetics in nanoscale water films, *Recent Res. Devel. Phys. Chem.* 1, 209-219, 1997.
- Smith, S.M., J.K. Wilson, J. Baumgardner, and M. Mendillo, Discovery of the distant Lunar sodium tail and its enhancement following the Leonid meteor shower of 1998, *Geophys. Res. Lett.* 26, 1649, 1999.
- Smyth, W.H. and M.L. Marconi, Theoretical overview and modeling of the sodium and potassium atmospheres of Mercury, *J. Astrophys.* 441, 839-864, 1995a.
- Smyth, W.H. and M.L. Marconi, Theoretical overview and modeling of the sodium and potassium atmospheres of the Moon, *J. Astrophys.* 443, 371-392, 1995b.
- Spencer, J.R. and A. Klesman, New observations of molecular oxygen on Europa and Ganymede, *Bull. AAS.*, #47.04, 1125, 2001.
- Sprague, A.L., A diffusion source for sodium and potassium in the atmospheres of Mercury and the Moon, *Icarus* 84, 93-105, 1990.
- Sprague, A.L., Mercury's atmospheric bright spots and potassium variations: A possible cause, *J. Geophys. Res.* 97, 18257-18264, 1992.
- Sprague, A.L., R.W.H. Kozlowski, D.M. Hunten, W.K. Wells, and F.A. Grosse, The sodium and potassium atmosphere of the Moon and its interaction with the surface, *Icarus* 96, 27-42, 1996.
- Sprague, A.L., R.W. Kozlowski, D.M. Hunten, N.M. Schneider, D.L. Domingue, W.K. Wells, W. Schmitt, and U. Fink, Distribution and abundance of sodium in Mercury's atmosphere, 1985-1988, *Icarus* 129, 506-527, 1997.
- Sprague, A.L., W.J. Schmitt, and R.E. Hill, Mercury: Sodium atmospheric enhancements, radar-bright spots, and visible surface features, *Icarus* 136, 60-68, 1998.
- Stern, S.A., The Lunar Atmosphere: History, status, current problems, and context, *Rev. Geophys.* 37, 453-491, 1999.
- Stern, S.A. and B.C. Flynn, Narrow-field imaging of the lunar sodium exosphere, *J. Astron.* 109, 835-841, 1995.
- Stern, S.A., A. Fitzsimmonds, R.M. Killen, and A.E. Potter, A direct measurement of the sodium temperature in the Lunar atmosphere, In *Lunar Planet. Sci. XXXI abstract 1112*, Lunar Planet Inst., Houston TX (CD-ROM) 2000.
- Stevenson, D.J., Volcanism and igneous processes in small icy satellites, *Nature* 298, 142-148, 1982.
- Stirniman, M.J., C. Huang, R.S. Smith, S.A. Joyce, and B.D. Kay, The adsorption and desorption of water on single crystal MgO(100): The role of surface defects, *J. Chem. Phys.* 105, 1295-1298, 1996.
- Strazzukka, G., Chemistry of ice induced by energetic charged particles, In *Solar System Ices* (ed. B. Schmitt et al., Kluwer, Netherlands) p. 281-302, 1998.
- Trafton, L., A two-component volatile atmosphere for Pluto, I - The bulk hydrodynamic escape regime, *Astrophys. J.* 359, 512-523, 1990.
- Vidal, R.A., D.A. Bahr, R.A. Baragiola, and M. Peters, Oxygen on Ganymede: laboratory studies, *Science* 276, 1839-1842, 1997.
- Walters, M., W.A. Jesser, J.W. Boring, and R.E. Johnson, Crystallization of SiO by He bombardment, *Radiat. Res.* 106, 189-201, 1988.
- Westley, M.S., R.A. Baragiola, R.E. Johnson, and G.A. Baratta, Ultraviolet photodesorption from water ice, *Planet. Space Sci.* 43, 1311-1315, 1995.
- Wiens, R.C., D.S. Burnett, W.F. Calaway, C.S. Hansen, K.R. Lykke, and M.L. Pellin, Sputtering products of sodium sulfate: Implications for Io's surface and for sodium bearing molecules in the Io torus, *Icarus* 128, 386-397, 1997.
- Wilson, J.K., S.M. Smith, J. Baumgardner, and M. Mendillo, Modeling an enhancement of the lunar sodium tail during the Leonid meteor shower of 1998, *Geophys. Res. Lett.* 26, 1645, 1999.
- Yakshinskiy, B. and T. Madey, Electronic desorption of Na from silicates, *Nature* 400, 642-644, 1999.
- Yakshinskiy, B.V., T.E. Madey, and V.N. Ageev, Thermal Desorption of Sodium Atoms from Thin SiO<sub>2</sub> Films, *Surface Rev. and Lett.* 7, 75-87, 2000.
- Yakshinskiy, B.V. and T.E. Madey, Electron and photon-simulated desorption of K from an ice surface, *J. Geophys. Res.* in press 2001.
- Zolotov, M.Y. and E.L. Shock, The composition and stability of salts on the surface of Europa and their oceanic origin, *J. Geophys. Res.* in press 2001.
- Zook, H.A. and J.E. McCoy, Large scale lunar horizon glow and high altitude lunar dust exosphere, *Geophys. Res. Letts.* 18, 2117-2120, 1991.